FULL PAPER

Light-Controlled Reversible Manipulation of Microgel Particle Size Using Azobenzene-Containing Surfactant

Yuriy Zakrevskyy, Marcel Richter, Svitlana Zakrevska, Nino Lomadze, Regine von Klitzing, and Svetlana Santer*

The light-induced reversible switching of the swelling of microgel particles triggered by photo-isomerization and binding/unbinding of a photosensitive azobenzene-containing surfactant is reported. The interactions between the microgel (*N*-isopropylacrylamide, co-monomer: allyl acetic acid, crosslinker: *N*,*N*′-methylenebisacrylamide) and the surfactant are studied by UV-Vis spectroscopy, dynamic and electrophoretic light scattering measurements. Addition of the surfactant above a critical concentration leads to contraction/collapse of the microgel. UV light irradiation results in *trans-cis* isomerization of the azobenzene unit incorporated into the surfactant tail and causes an unbinding of the more hydrophilic *cis* isomer from the microgel and its reversible swelling. The reversible contraction can be realized by blue light irradiation that transfers the surfactant back to the more hydrophobic *trans* conformation, in which it binds to the microgel. The phase diagram of the surfactant-microgel interaction and transitions (aggregation, contraction, and precipitation) is constructed and allows prediction of changes in the system when the concentration of one or both components is varied. Remote and reversible switching between different states can be realized by either UV or visible light irradiation.

1. Introduction

Gel based materials have initiated many scientific activities directed to understand their physical properties and exploration of application potentials.[1] The driving force of the developments in this field is unique swelling behavior of hydrogels which can change in response to surrounding conditions (temperature, pH, ionic strength, solvent).[2] Polymer gels react on local environmental variations by changing their size, an important factor in micro-fluidic devices and micro-sensors developments.[1a,3] Stimuli responsive gels have been also intensively explored for applications in biology and medicine.[4] They were proposed for use as carriers of therapeutic drugs,[1d,2d,5] biosensors,[6] and active materials in artificial muscles,[7] wound dressing,[8] tissue engineering,[9] and contact lenses.[10]

The most useful feature of a hydrogel for the success in application is the realization of remote control by external stimuli such as light, electric or magnetic field. Light is seen as the most desirable stimulus because it can be virtually delivered to practically any microscopically sized site using modern fiber optic technology. To realize remote control of a hydrogel by driving the polymer through a transition process (e.g., swelling transition, glass transition) a variety of nanoparticles (e.g., silicate, metal, magnetic, or carbon nanotubes) were incorporated into polymer networks.[11] The underlying idea is that nanoparticles can absorb specific stimuli (e.g., alternating magnetic fields, near-IR light) and generate heat.[11b] The success of nanocomposites was so immense that practically no effort was made to develop alternative control approaches except for the attempt to generate heat by direct high intensity irradiation of PNIPAM based gel.[12] For temperature as a local stimulus nanocomposites are indeed the most successful strategy.

Recently it was shown that the reversible light-induced volume swelling of PNIPAM gels can be realized if spirobenzopyran derivatives are covalently incorporated into the gel structure.[13] Although this approach does not require nanoparticles, the microgel structure must be modified chemically. The only attempt of nonreversible control of microgel de-swelling without its chemical modification was achieved using photodegradable surfactant.[14]

To realize completely reversible light controlled manipulation of microgel swelling properties we propose to use a photosensitive azobenzene-containing surfactant (**Figure 1**a). Its hydrophobic-hydrophilic properties can be reversibly tuned by light through reversible *trans-cis* photo-isomerization transition of the azobenzene unit (Figure 1b). The microgel particles are based on NIPAM (chemical composition is shown in Figure 1c), which is characterized by its lower critical solution

Dr. Y. Zakrevskyy, S. Zakrevska,
Dr. N. Lomadze, Prof. S. Santer
Experimental Physics
Institute of Physics and Astronomy
University of Potsdam
Karl-Liebknecht-Str. 24/25, 14476 Potsdam, Germany
E-mail: yuriy.zakrevskyy@uni-potsdam.de
M. Richter, Prof. R. von Klitzing
Applied Physical Chemistry
Institute of Chemistry
Technical University Berlin
Straße des 17. Juni 124, 10623 Berlin, Germany

DOI: 10.1002/adfm.201200617

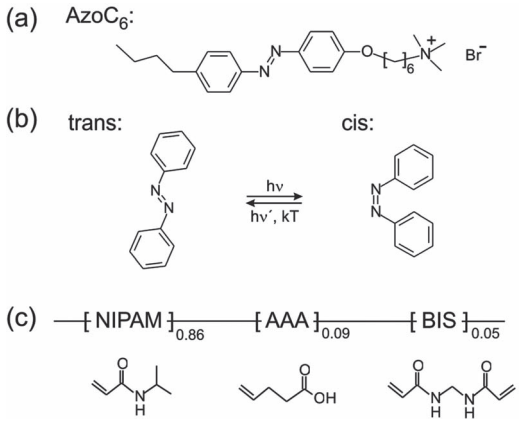

Figure 1. (a) Chemical structure of the photosensitive azobenzene containing surfactant: **AzoC$_6$**. (b) Light-induced isomerization of the azobenzene unit. (c) Schematic representation of the chemical composition of the microgel particles: **NIPAM-AAA-BIS**.

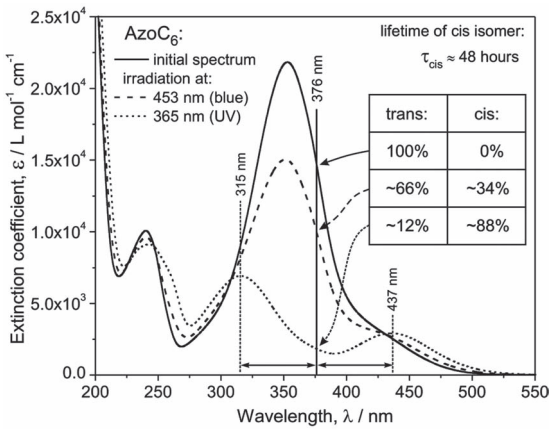

Figure 2. Extinction spectra of the azobenzene-containing surfactant (AzoC$_6$) in pure water solution measured at the concentration of $5 \cdot 10^{-5}$ M, which is below CMC (~0.5 m M). The spectra after UV and visible irradiation for 10 minutes in each case correspond to saturation, or so-called steady state. Isomeric composition after each irradiation, determined from the absorption at 376 nm, is given in the table.

temperature (LCST) of around 32 °C, meaning that the polymer network exists in a swollen state below this LCST.[15] The incorporation of organic acids, like acryl acid (AAc) or allyl acetic acid (AAA), leads along with thermo-responsive behavior to pH-sensitivity.[16] Microgels containing co-monomer differ in their mechanical and swelling behavior compared to those without co-monomer.[17] In this article we report on interaction between the microgel particles and the surfactant, contraction of the particle as a result of this interaction, and light-induced reversible manipulation of the contraction behavior.

During preparation of this manuscript investigation of a very similar complex was published.[18] It was demonstrated that binding of photosensitive surfactant to microgel can be reversed by UV light irradiation; the system returns to the initial state after 2 days relaxation in the dark. In the present paper we demonstrate all-optical and completely reversible control of the microgel swelling/contraction process by changing the irradiation wavelength. It should be noted that we have also investigated microgel containing AAc and found that the response of the microgel is more pronounced if more hydrophobic AAA was used. Moreover, here it is shown that employment of the surfactant with longer alkyl tail attached to azobenzene results into tenfold decrease of the surfactant concentration needed to trigger the interaction. Detailed investigation of the complex at different microgel concentration allows construction of the phase diagram, which enables understanding of the transitions mechanisms and selection of appropriate conditions for realization of the light-induced reversible control of the microgel swelling properties.

2. Results and Discussion

2.1. Photo-Isomerization Behavior of the Surfactant

To achieve light-induced manipulation of the surfactant behavior in water solution an azobenzene unit was incorporated into the hydrophobic tail of the surfactant (see Figure 1a). It is well known that azobenzene is the most efficient and extensively investigated photosensitive unit, which shows reversible light-induced switching between *trans*- and *cis*-isomers (Figure 1b).[19] The thermodynamically stable *trans* isomer is more hydrophobic (dipole moment across the azo-linkage: ~0.5 D) whereas the *cis* isomer is more hydrophilic (dipole moment: ~3.0 D). Both isomers of the surfactant possess characteristic absorption bands in their UV-Vis spectra presented in **Figure 2**. In the dark, the surfactant is predominantly in the *trans* form. The *trans-cis* isomerization can be achieved by UV light irradiation and the reversible reaction can be realized either by blue light irradiation or thermal relaxation in the dark with the characteristic lifetime of about two days. Due to such long life time, the spectra do not change considerably after the irradiation is turned off. The presented spectra after irradiation for several minutes correspond to the saturation, or so-called steady state, where further irradiation does not result in spectral changes. Exposure to UV light of around 365 nm leads to conversion of mostly all isomers to the *cis* configuration, although there is some residual amount of the surfactant in the *trans* form. The extinction coefficient at 376 nm of the dark state spectrum, exactly between the peaks of the *cis*-form where its absorption is supposed to be minimal, was used to estimate the amount of *trans* isomers in solution after isomerization process. Assuming that the initial state corresponds to pure *trans* form of the surfactant, the isomeric composition for each irradiation was calculated and is shown in the inset table in Figure 2. Irradiation with blue light at 453 nm does not result in a complete transition to the initial dark state, because at this wavelength both isomers absorb light and the steady state depends on the ratio of the corresponding extinction coefficients of both isomers at the chosen excitation wavelength. Therefore, about 1/3 of the surfactant molecules still remain in the *cis* state.

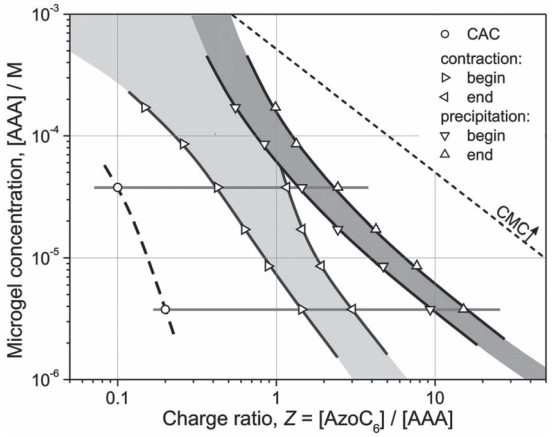

Figure 3. Phase diagram of the complex between microgel particles (NIPAM-AAA-BIS) and the photosensitive surfactant ($AzoC_6$). Charge ratio Z is the molar ratio between concentrations of $AzoC_6$ and AAA groups of the particles.

2.2. Phase Diagram of the Microgel-Surfactant Complex

To facilitate the discussion and understanding of the experiments in the following sections it is apt to present the phase diagram of the complex formation and its behavior without irradiation of the surfactant (see **Figure 3**). The phase diagram was constructed using the results presented below. To observe changes in the order of two or more magnitude, it is necessary to plot the phase diagram in log-log scale.[20] The ordinate is the concentration of carboxylic groups, or allyl acetic acid (AAA) chains, of the microgel. As the deprotonation of this group might depend on the overall as well as surfactant concentrations, the total nominal concentration is used (see Experimental section for details). The abscissa is the charge ratio Z, which is the molar ratio of the surfactant (its positive charge) and the carboxylic groups (their potential negative charge) of the microgel. In this scaling the critical micelle concentration (CMC) of the surfactant in water is represented by a line in the phase diagram. This line and all lines parallel to it correspond to a constant surfactant concentration. Notably, all experiments were carried out below CMC to avoid influences caused by micelle formation.

In Figure 3 the horizontal gray lines correspond to [AAA] concentrations equal to $3.8 \cdot 10^{-5}$ M and $3.8 \cdot 10^{-6}$ M, respectively. These are the two representative concentrations for which the detailed investigation was carried out. Some experiments were repeated for other concentration to complete the phase diagram. For a fixed microgel concentration, i.e. fixed value of [AAA], and increasing amount of the surfactant, i.e the charge ratio Z, several transitions can be seen in Figure 3. Increasing Z from zero one reaches at first the critical aggregation concentration (CAC), the concentration at which the surfactant starts to bind to the gel particles. On further increase of the surfactant concentration the contraction range is reached indicated by the start and end lines. There is also a range where the precipitation of the complex takes place. The contraction range is broadening at higher microgel concentrations leading to overlap of the contraction and the precipitation ranges at [AAA] > $5 \cdot 10^{-5}$ M. Having the general picture of the processes, the experimental result on interactions between the components in the complex can be discussed in detail.

2.3. Binding of the Surfactant to the Microgel and its Effect on the LCST

To assess the binding charge ratio of the $AzoC_6$ surfactant to the microgel UV-Vis spectra of the residual surfactant solutions (the supernatant after centrifugation of the complex) were measured. The surfactant concentration was calculated using its extinction spectrum without irradiation. Comparison of these spectra and the spectrum of pure surfactant showed that they are mostly identical and proved that no microgel was left in the residual solution after centrifugation. The results for microgel concentration of [AAA] = $3.8 \cdot 10^{-5}$ M are shown in **Figure 4**a. It

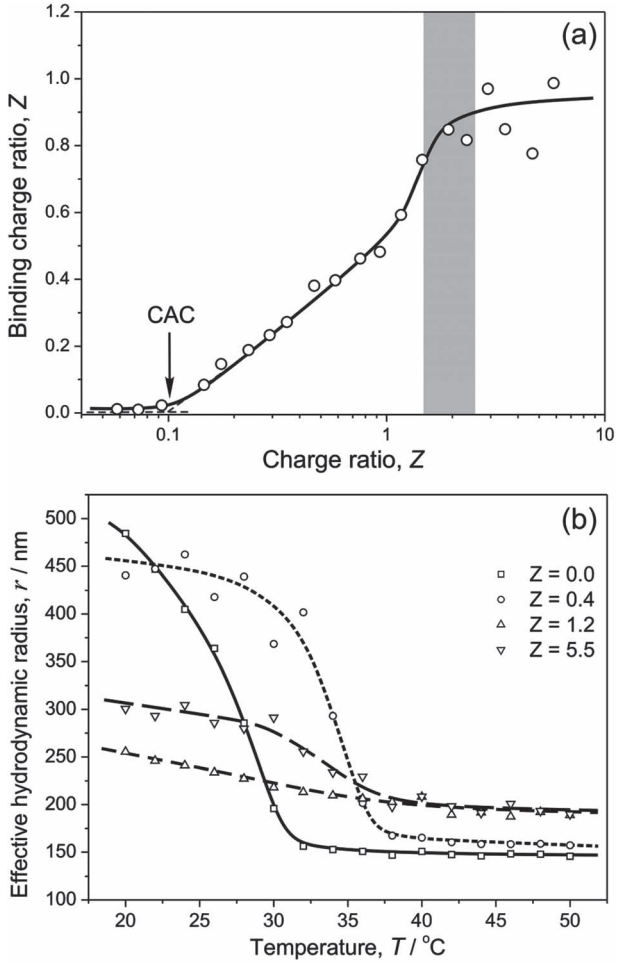

Figure 4. (a) Binding charge ratio of the surfactant determined from UV-Vis spectra after centrifugation versus the mixing charge ratio of the complex. The onset of binding is identified as critical aggregation concentration (CAC). (b) Temperature-induced changes of the hydrodynamic radius determined with dynamic light scattering of the microgel particles in complex with the surfactant for different mixing charge ratios Z. The concentration of the microgel in (a) and (b) is [AAA] = $3.8 \cdot 10^{-5}$ M.

is seen that the binding between surfactant and microgel starts only when some critical amount of $AzoC_6$ is added. The concentration of the surfactant at which the binding starts is assigned to the critical aggregation concentration (CAC). Starting from this point, the bound amount of the surfactant rises logarithmically with increasing the total surfactant concentration; note the log scale of the abscissa. There is a small increase of the binding charge ratio in the precipitation range, which is indicated by a grey region in the figure, and saturation in the colloidally stable range. The same experiment, carried out for lower concentration of the microgel [AAA] = $3.8 \cdot 10^{-6}$ M, showed similar behavior. The values of CAC for both microgel concentrations are shown in the phase diagram in Figure 3. The transition line is not parallel to the CMC line, which corresponds to the constant surfactant concentration, indicating dependence of the CAC on the microgel concentration. The binding starts far before the onset of the contraction proving that some amount of the negative charges in the gel should be compensated to initiate the contraction process.

The temperature induced volume phase transition, which is inherent in the NIPAM co-polymer, was studied for different charge ratios Z. The following probes with microgel concentration [AAA] = $3.8 \cdot 10^{-5}$ M were selected for this experiment (cf. Figure 3): Z = 0.0 (pure microgel), Z = 0.4 (just at the line of the contraction begin), Z = 1.2 (at the line of the contraction end), and Z = 5.5 (in the colloidally stable range). The respective temperature dependent effective hydrodynamic radius measurements are shown in Figure 4b. The point of deflection (lower critical solution temperature: LCST) for pure microgel is at 28 °C, i.e. a bit lower than 32 °C, the typical LCST for pure PNIPAM microgel. Although the presence of charges leads to increase of the LCST,[17] AAA has also a hydrophobic effect which can result in the LCST reduction. After addition of the surfactant above CAC but still below the concentration where the surfactant initiated contraction takes place (Z = 0.4), the LCST is shifted to higher temperatures by 7 °C. The impact of the surfactant on the LCST is an indication that the surfactant penetrates into the microgel particles and stabilizes it. Driven by ionic as well as hydrophobic forces, the surfactant molecules might bind to the polymer chains and add stiffness to the network; the surfactant might also make bridges between neighbor chains. Note the increase of the contracted particle size at elevated temperature above 40 °C that is assigned to the presence of the bound surfactant. In the surfactant induced contracted state (Z = 1.2) the temperature initiated volume phase transition is rather blocked; there is only small change of the slope around 35 °C. The hydrodynamic radius at elevated temperatures increases further because of the surfactant binding. The transition reappears for the colloidally stable system (Z = 5.5) but the size at elevated temperatures does not increase any more indicating saturation of the amount of the bound/trapped surfactant. As the colloidal stability is achieved by binding of the surfactant to the contracted hydrophobic microgel, discussed in the following section, the larger effective hydrodynamic radius at room temperature can be assigned to the effect of the stabilizing shell. This stabilizing surfactant layer might be partially removed during the temperature induced volume phase transition.

2.4. Spectroscopic Study of the Complex in the Precipitation and Colloidally Stable Ranges

Six series of complexes each having fixed microgel concentration and varying charge ratios Z were prepared. In each series there was a range of Z where the formation of precipitate was visually observed. For higher microgel concentrations the precipitate was observed just after mixing; for lower concentration larger initial volumes were necessary to see the precipitation. All samples were left to equilibrate at room temperature for at least 24 hours to allow the precipitate to settle down. No centrifugation was done to avoid the removal of colloidally stable complex. The top part of each sample was then carefully taken to characterize the residual composition using UV-Vis spectroscopy. The results for [AAA] = $3.8 \cdot 10^{-5}$ M are shown in **Figure 5**a as an example. The microgel (Z = 0.0) absorbs only in the UV range and only the shoulder of the absorption band located in deep UV can be measured. Addition of surfactant up

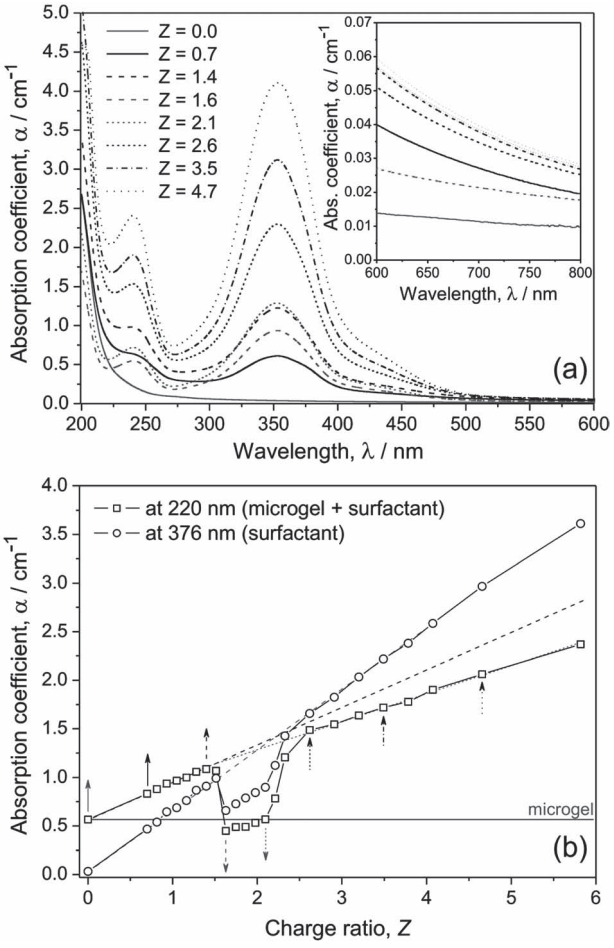

Figure 5. (a) UV-Vis spectra of the microgel and its complexes with the surfactant of different charge ratios Z. Inset: The corresponding changes of light scattering in the long-wavelength range. (b) Absorption coefficient at 376 nm (surfactant) and 220 nm (microgel + surfactant) versus Z. A considerable drop of absorption in the range of precipitate formation 1.5 < Z < 2.4 can be observed. The arrows correspond to the spectra in (a). The concentration of microgel is [AAA] = $3.8 \cdot 10^{-5}$ M.

to Z = 1.5 results effectively to the sum of the spectra of both components. However, in the precipitation range (1.5 < Z < 2.4) there is a considerable drop of the absorption. These changes are better seen if the absorptions at 376 nm (absorption of the surfactant) and at 220 nm (absorption of the microgel + surfactant) is plotted as a function of Z (see Figure 5b). To track the surfactant concentration its peak absorption at 353 nm could be used. However, to be consistent with the experiments under irradiation presented below, the absorption at 376 nm was employed. Since for non-irradiated surfactant both absorptions are proportional the observed changes differ only by a constant factor defined by a ratio of the extinction coefficients at these wavelengths. There is no spectral range where only microgel absorbs; thus, to track the changes in the microgel concentration the absorption at 220 nm, at which the surfactant has a minimum, was used. It is seen from Figure 5b that in the precipitation range (1.5 < Z < 2.4) the absorption at 220 nm drops below the level of pure microgel. The gel and the surfactant bind together and precipitate from the solution. However, starting from Z > 2.4 both components are again present in the spectra and no precipitate was visually detected; this indicates that the complex becomes colloidally stable. The same experiments were carried out for other microgel concentrations to identify the points of begin and end of the precipitation range. The results are shown in the phase diagram in Figure 3.

To clarify the role of the surfactant and, in particular, its isomeric composition in the colloidal stabilization of the complex the following experiment was conducted. For the concentration of the microgel of [AAA] = $3.8 \cdot 10^{-5}$ M, colloidally stable complexes with Z > 2.4 were exposed to UV light to induce *trans-cis* isomerization of the surfactant. The samples were irradiated with small doses and after each irradiation step a UV-Vis spectrum was collected. During irradiation, typical *trans-cis* isomerization behavior in the UV-Vis spectra up to some irradiation dose was observed (spectrum after 60 s irradiation in **Figure 6**a). Starting from this point, the next irradiation step resulted in a pronounced increase of the scattering and precipitation which was visually observed. Further irradiation after the precipitation onset led to a decrease of scattering and absorbance. This can be explained by the formation of large aggregates, which settle on the bottom of a cuvette and do not scatter and absorb light.

The irradiation dose before the precipitation onset increased with Z, suggesting that more surfactant molecules had to be converted to the *cis* state to reach the precipitation point. To understand this behavior, the spectra of samples with Z > 2.4 just before the onset of precipitation were plotted together (Figure 6b). It is clearly seen that the absorption coefficient near 376 nm is the same for all spectra. The absorption at this wavelength corresponds to the *trans* isomer (see section 2.1); therefore, at the precipitation point the concentration of the surfactant in *trans* conformation is the same. The extinction coefficient at 376 nm was used to assess the concentration of the surfactant in *trans* form, which was about 9.1×10^{-5} M. Division by the microgel concentration ([AAA] = $3.8 \cdot 10^{-5}$ M) gave the charge ratio between the *trans* isomer and the microgel $Z_{precipitation}^{trans-} \approx 2.4$, which is the same as the value where the precipitation range ends (Z = 2.4). The fact that this value is the same for all samples, which have different initial mixing charge ratios, proved that only the *trans* isomer of the surfactant is responsible for the colloidal stability. The precipitation will take place if the charge ratio of *trans* isomers to [AAA] is smaller than $Z_{precipitation}^{trans-}$.

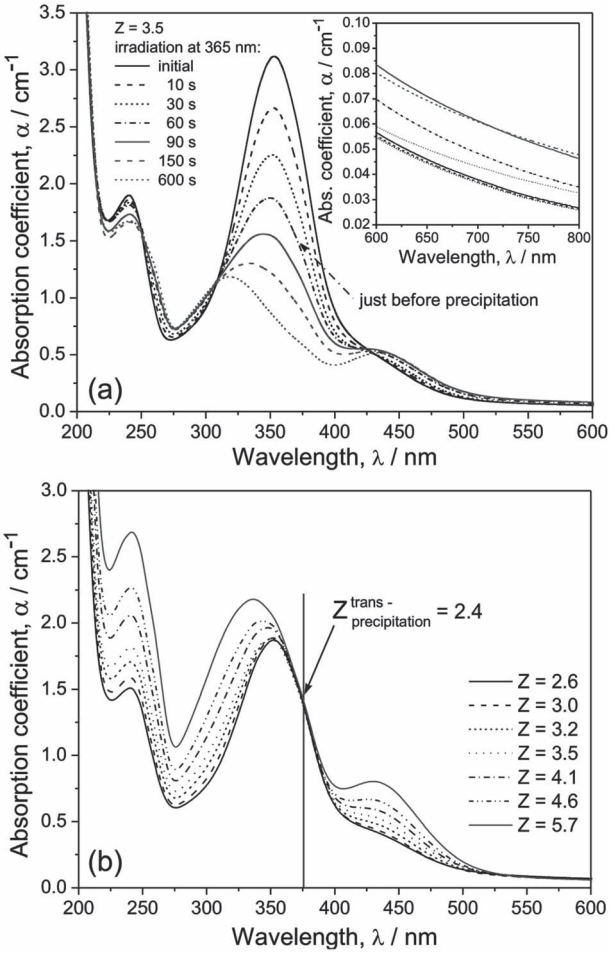

Figure 6. (a) Changes in UV-Vis spectra of the microgel-surfactant complex (Z = 3.5, [AAA] = $3.8 \cdot 10^{-5}$ M) during UV light irradiation. Inset: The corresponding changes of light scattering in the long-wavelength range. (b) Spectra of the complexes for Z > 2.4, which were irradiated by UV light, measured just before the onset of precipitation.

2.5. Dynamic Light Scattering Characterization of the Contraction and Precipitation Ranges

2.5.1. Experiments without Irradiation

To understand the precipitation and stabilization behavior of the complexes, zeta-potential was measured for two series with microgel concentrations of [AAA] = $3.8 \cdot 10^{-5}$ M and $3.8 \cdot 10^{-6}$ M, and a changing charge ratio Z. The results are shown in **Figure 7**a. The zeta-potential is negative for small values of Z up to the onset of precipitation that is consistent with the stability of the system because the particles are negatively charged coming from the co-monomer AAA and the radical starter KPS. Just before the precipitation, there is an abrupt increase of the zeta-potential, which crosses the zero point in the precipitation

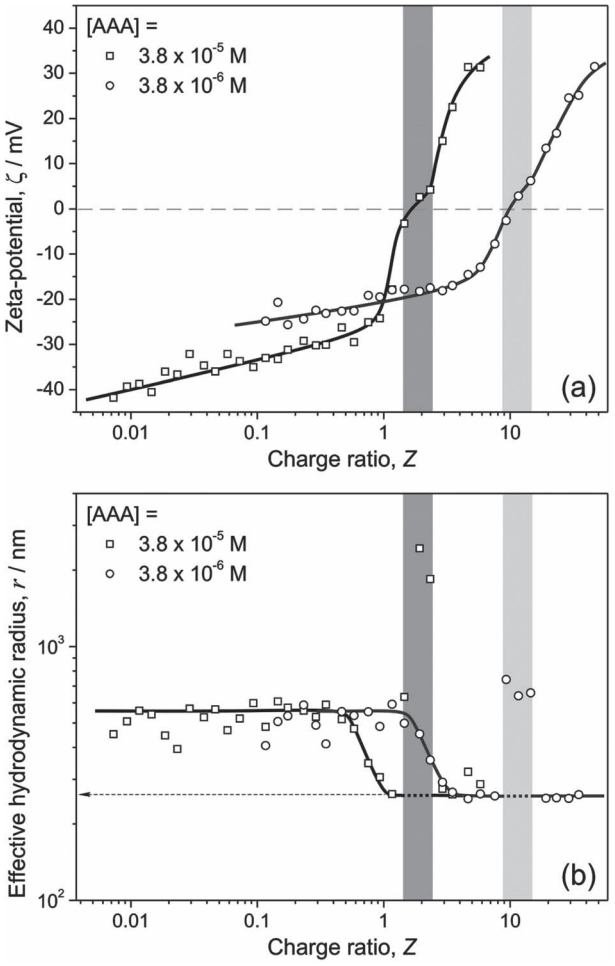

Figure 7. Changes of (a) zeta-potential and (b) effective hydrodynamic radius of the microgel-surfactant complexes as a function of charge ratio Z for two series of complexes of fixed microgel concentrations. The precipitation ranges are marked by the correspondingly gray rectangles.

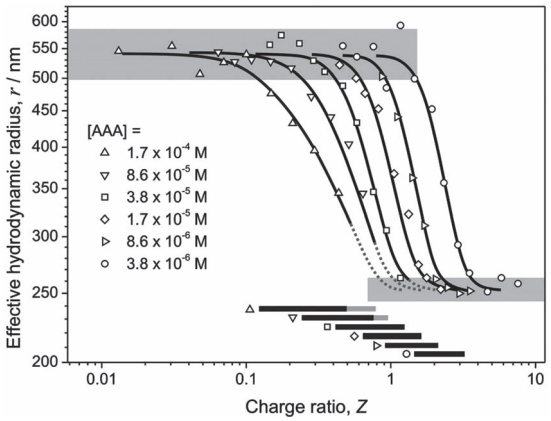

Figure 8. Effective hydrodynamic radius of the complexes as a function of charge ratio Z for different microgel concentrations. The contraction ranges are marked by the corresponding bars.

range. This is an indication that the bulk and surface charge of the microgel is completely compensated by the bound positively charged surfactant. The particles are neutral and experience hydrophobic attraction force between each other leading to precipitation. Further addition of the surfactant in the *trans* conformation leads to its binding to the hydrophobic particles. They become positively charged and colloidally stable.

For the same series the effective hydrodynamic radius was measured (see Figure 7b). The large scattering in the values of the radius for small Z can be explained by flexibility of the microgel in the swollen state. With the onset of contraction the fluctuation of the size measurement becomes much smaller. In the precipitation range only the residual amount of particles was characterized; the scattering in the radius measurement was very large. There are two essential features which should be noted in the dynamic light scattering experiment: (i) the contraction process does not coincide and always precedes the precipitation range, (ii) there is no influence of the contraction on the zeta-potential (cf. Figure 7a). This behavior can be explained as follows; the contraction process starts when certain amount of the surfactant is bound to the microgel leading to a compensation of the bulk charge of deprotonated AAA groups in the gel. This does not exclude the existence of the surface charges on microgel particles, which is responsible for the existence of the zeta potential. The surfactant molecules diffuse at first into the microgel to compensate its bulk charge and then after saturation and contraction bind to the surface.

The Z-dependent effective hydrodynamic radius measurements were carried out for different concentrations of the microgel (**Figure 8**). The particle radius decreases more than twice on addition of the surfactant that corresponds to an about tenfold decrease of the volume. The transition shifts to larger values of Z with dilution of the complex indicating that more surfactant should be added to initiate the transition. The contraction range was identified by start and end points, where the clear deviation (~5–10%) from the average value in the corresponding plato was observed. In Figure 8 the contraction ranges are marked by the corresponding bars. For the two highest microgel concentrations, because of precipitation, it was impossible to detect the end of contraction. The obtained values were used to confine the contraction range in the construction of the phase diagram (Figure 3).

2.5.2. Light-Induced Changes

Zeta-potential and effective hydrodynamic radius measurements were carried out before and after irradiation for selected probes from two series of fixed microgel concentrations of [AAA] = $3.8 \cdot 10^{-5}$ M and $3.8 \cdot 10^{-6}$ M and a changing charge ratio Z. The complexes were at first irradiated by blue light (453 nm) and then they were exposed to UV light (365 nm). Irradiation for several minutes was sufficient to reach the steady state, as was confirmed by UV-Vis spectroscopic measurements. Absorption at 376 nm was used to estimate the quotients of each isomer after irradiation; these values were very close to those of pure surfactant (see inset table in Figure 2). The light-induced changes of zeta potential are shown in **Figure 9**a. Note, that the large changes in zeta potential take place near the precipitation

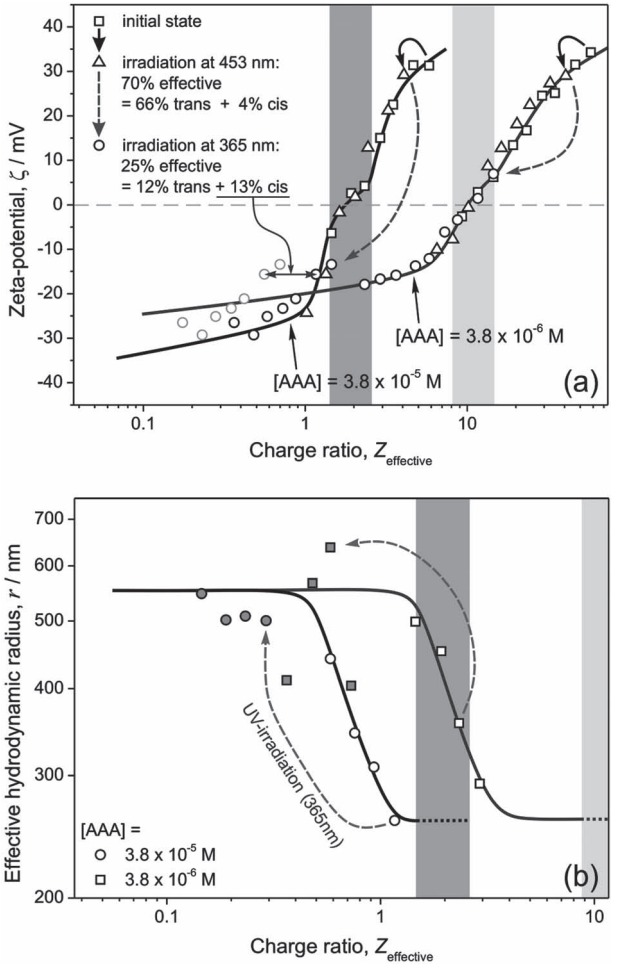

Figure 9. Changes of (a) zeta-potential and (b) effective hydrodynamic radius of the complexes as a function of effective charge ratio $Z_{effective}$ for two series of complexes of fixed microgel concentration after irradiation by blue and UV light. For the details of calculation of the effective charge ratios see text. The precipitation ranges are marked by the correspondingly gray rectangles. The arrows show the changes of either zeta-potential or effective hydrodynamic radius for the same sample after irradiation.

range. Therefore, probes in the precipitation and colloidally stable ranges were selected for this experiment. To simplify the understanding of the changes under irradiation, the tendency line of the zeta-potential vs. charge ratio for non-irradiated complexes (see Figure 7a) was used.

To understand the data processing the issue of effective charge ratio after irradiation must be discussed. Ideally, the more hydrophobic *trans* isomer shows a much stronger binding ability to the microgel than the more hydrophilic *cis* form of the surfactant. If only surfactant molecules in the *trans* conformation affected the values of zeta-potential, the values of $Z_{effective}$ would be 66% and 12% of the corresponding initial charge ratio after blue and UV light irradiation respectively (see inset table in Figure 2). The calculation using these values was done but the zeta-potential values were shifted to the left with respect to the tendency line (gray points for [AAA] = $3.8 \cdot 10^{-5}$ M after UV irradiation are shown as an example in Figure 9a). This was an indication that surfactant molecules in the *cis* conformation also affect the values of zeta-potential. Therefore, to adjust the points to the tendency line the values of $Z_{effective}$ were increased to 70% (66% of *trans* + 4% of *cis* isomer) for the blue light irradiated samples. For the UV light irradiation one must already add 13% of *cis* isomer to the effective charge ratio to get $Z_{effective}$ = 25% (12% of *trans* + 13% of *cis* isomer) to account for the changes in zeta-potential. Note that in the latter case the quotient of the surfactant converted to the *cis* form is much larger. These are approximate correction values and should not be taken literally. The main conclusion from this experiment is that the *cis*-surfactant also takes part in the complex formation; its effect is much smaller but should not be underestimated. One might think of the effective charge ratio as the equivalent ratio of the surfactant in the dark state that produces the same changes in complex properties.

For the light-induced changes of effective hydrodynamic radius the samples from the contraction range were selected. The results for two series of fixed microgel concentration are plotted in Figure 9b, where the tendency lines of the contraction process are also shown (cf. Figure 7b). It is seen that partially and completely contracted particles swell under irradiation with UV light. The swollen particles are very flexible leading to uncertainties in the measurement of the hydrodynamic radius, as already discussed above. The effective charge ratio $Z_{effective}$ was calculated using the results from the above zeta-potential experiment. Note that the irradiation not only results in re-swelling of the microgel, but the precipitated complex can also be re-dissolved if $Z_{effective}$ is smaller than the corresponding Z value at the line where the precipitation begins.

2.6. Light-Induced Reversibility

After clarifying the mechanisms of contraction, precipitation, and colloidal stabilization, reversibility of light-induced swelling/contraction transition was investigated. The surfactant steady state, i.e. the *trans*/*cis* composition, should be considered to realize the completely reversible process. From the spectra in Figure 2 one can see that irradiation with blue light does not return the surfactant into its initial dark state. For this reason, if completely contracted complex particle with Z close to the edge of the contraction end is taken and irradiated by UV light to induce swelling, the irradiation with blue light might not result into the reversible contraction. One should take into account that after irradiation by UV light $Z_{effective}$ is about 25% and after blue light irradiation it is already around 70% of the initial value.

To realize the light-induced reversibility a sample in the precipitation range with Z = 1.7 and [AAA] = $3.8 \cdot 10^{-5}$ M was prepared. It was then exposed to UV light to re-dissolve the precipitated complex. Then the complex was irradiated by blue light ($Z_{effective} = 1.7 \cdot 70\% = 1.2$) to induce the microgel contraction or by UV light ($Z_{effective} = 1.7 \cdot 25\% = 0.43$) to induce its reversible swelling. The expected values of the effective charge ratios after each irradiation lay close to the corresponding contraction beginning and end lines (cf. Figure 3). The light-induced reversible changes in microgel size are shown in **Figure 10**. By this

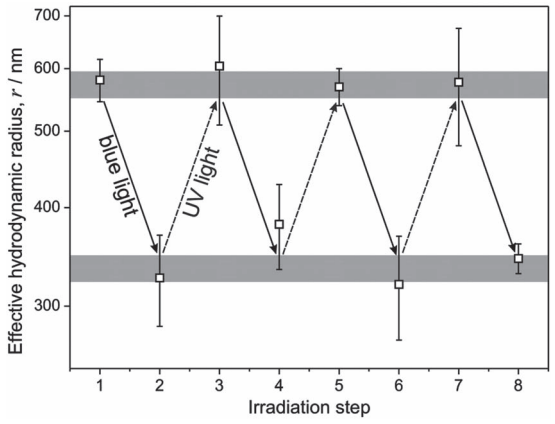

Figure 10. Reversible changes of the effective hydrodynamic radius for the sample with Z = 1.7 and [AAA] = $3.8 \cdot 10^{-5}$ M after blue light (even irradiation step) and consequent UV light (odd irradiation step) irradiation.

experiment we demonstrate for the first time that by switching between UV and blue light irradiation completely reversible all optical contraction/swelling transition of the microgel can be realized.

2.7. Model of the Light-Induced Contraction/Swelling Process

Finally, we present the model of reversible light-controlled manipulation of microgel swelling that is based on the result presented above. The schematic representation of the process is presented in **Figure 11**. After mixing of the surfactant and the microgel particles in appropriate ratio, the complex formation between both components is attributed to combined electrostatic and hydrophobic attraction. This process takes place if the concentration of the surfactant exceeds some value, which is called critical aggregation concentration (CAC). Surfactant molecules with hydrophobic tail in the *trans* configuration diffuse into the microgel and compensate its charge. If the effective charge in a particle is reduced to some critical value, the contraction starts and goes on with further addition of the surfactant until saturation. When the contracted microgel-surfactant complex is irradiated by UV light, causing the transition of azobenzene unit to the *cis* configuration, the tail of the surfactant becomes hydrophilic. This reduces hydrophobic forces, which essentially have entropic origin, between bound surfactant molecules in the contracted microgel particle. Driven by entropy the surfactant molecules in the *cis* configuration start to unbind leading to de-swelling of the microgel. The contraction is realized by blue light exposure, which causes reversible *cis-trans* isomerization and binding of the surfactant in the *trans* configuration to the microgel. The process is all optical and completely reversible.

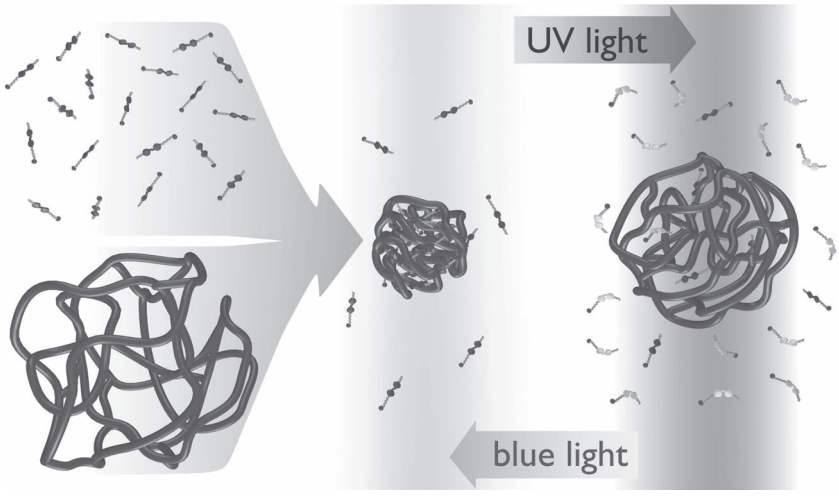

Figure 11. Schematic representation of interaction between microgel particle and photosensitive surfactant. UV light irradiation leads to *trans-cis* isomerization of the surfactant and unbinding of the *cis* isomer that result in de-swelling of the microgel. The reversible surfactant binding and microgel contraction is realized by blue light irradiation, which transforms the surfactant back to the *trans* conformation.

3. Conclusions

Reversibility of interactions between microgel particles and photosensitive azobenzene-containing surfactant caused by either UV or visible light irradiation of the complex was investigated in detail by UV-visible spectroscopy and dynamic light scattering measurement of hydrodynamic radius and zeta-potential. There is a critical aggregation concentration (CAC) at which the surfactant starts to bind to the microgel. The binding, which reduces the bulk charge in the microgel, has minor influence on the values of zeta-potential and the colloidal stability. The contraction, which is also not accompanied by pronounced zeta-potential changes, starts only when a critical amount of the surfactant is bound to the microgel. The complex remains colloidally stable even when the contraction is completed. This behavior is explained by the penetration of the surfactant into bulk of the gel particle. When the surfactant binding compensates the microgel surface charge, causing the hydrophobic attraction, the complex aggregates and precipitates from the solution. The precipitation can be prevented if more surfactant in the hydrophobic *trans* conformation is initially added to the solution.

The measurements of CAC, contraction and precipitation ranges were carried out for different microgel concentrations and varying mixing charge ratios, which equals to the surfactant concentration, or its positive charge, divided by concentration of carboxylic groups, or potential negative charge, in the microgel. Based on these results, the phase diagram of complex formation and its transitions was constructed. It can be used to predict the changes in the complex behavior when the concentration of one or both components is changed.

Irradiation of the surfactant by UV or visible light results in either *trans-cis* or *cis-trans* isomerization of the azobenzene unit

incorporated into its tail, respectively. The more hydrophobic *trans* isomer reduces the surfactant affinity to water whereas the more hydrophilic *cis* conformation leads to an increase of the affinity. In this way the hydrophobic interaction between the surfactant molecules can be tuned. In the presence of oppositely charged microgel the electrostatic attraction should be added to the hydrophobic forces. The possibility to manipulate with light the interactions between the surfactant and microgel is used to realize remote control of the hydrogel swelling/contraction behavior. Irradiation by UV light transfers the surfactant predominantly to the *cis* conformation and results to its unbinding and swelling of the microgel. The reversible contraction is realized by blue light irradiation converting the surfactant predominantly to the *trans* state, which binds to the microgel. This process is completely reversible. Notably that the *cis*-surfactant shows much weaker binding to the microgel than its *trans* counterpart; however, this interaction should not be underestimated if the concentration of the *cis* form is very high.

In conclusion, for the first time the light-induced reversibility of contraction/swelling behavior of microgel using photosensitive azobenzene containing surfactant was demonstrated, which can make competition to the well investigated nanocomposite systems. We believe, after corresponding optimization of the microgel and surfactant for particular application needs, such systems can find their use in drug delivery, artificial muscles, and micro-fluidic devices.

4. Experimental Section

Microgel: The monomer N-isopropylacrylamide (NIPAM, Aldrich, 97%), crosslinker N,N'-methylenebisacrylamide (BIS, Aldrich, 99,5%), the co-monomer allyl acetic acid (AAA, Aldrich, 97%) and the radical starter potassium persulfate (KPS, Fluka, 99%) were used without further purification. The obtained particles were synthesized via surfactant free emulsion polymerization.[7] NIPAM, BIS (5 mol% with respect to the mass of NIPAM) and AAA (50 mol% with respect to the mass of NIPAM) were dissolved in 100 mL Milli-Q water. The solution was heated to 70 °C under a constant nitrogen stream. After an equilibration time of 30 min, the polymerization was initiated by the addition of 1 mg KPS dissolved in 1 mL Milli-Q water. Within 10 min, the colorless solution turned into a milky emulsion. The reaction was stirred for 4 hours at 70 °C. Afterwards, the turbid solution was cooled down to room temperature and stirred over night. The microgel was dialyzed for 14 days with Milli-Q water to remove oligomers and unreacted educts. The water was changed daily. After the dialyse process, the particles were freeze-dried. The amount of incorporated AAA was determined by titration. For the titration a Titrando 836 from Metrohm was used. The titration was done as follows: 0.5 wt-% of the microgel was solved in Milli-Q water. The obtained solution was titrated against a 2.5 mM NaOH solution. From analysis of the data it was found that 9% of the AAA was effectively incorporated into the microgel particles.

Surfactant: An azobenzene-containing trimethylammonium bromide surfactants $AzoC_6$ (Figure 1b) was synthesized according to the procedure described in reference.[20] The surfactant critical micelle concentration (CMC) in pure water was determined by isothermal titration calorimetry and by a novel method using titration UV-Vis spectroscopy, to be ~0.5 mM.[21] All experiments were carried out below CMC to avoid influence of effects related to the micelle formation. No buffer solution was used to fix pH value because depending on a buffer and its concentration the CMC of the surfactant decreases dramatically as a result of change of the ionic strength.[21] Prior to the mixing with the microgel, the surfactant was kept in the dark for several days to ensure complete relaxation to the *trans* configuration. All experiments were carried out in a room with yellow light to avoid any isomerization of the surfactant.

Complexes: Deionized water (MilliQ) was used to prepare initial solutions of the microgel and the surfactant. Both $AzoC_6$ and microgel solutions were diluted prior to mixing to get a desired concentration of microgel (determined by the total concentration of carboxylic groups [AAA]) and a molar ratio of [$AzoC_6$] to [AAA] defined as $Z = [AzoC_6]/[AAA]$.

Methods: Irradiation of the surfactant alone or in complex with the microgel was done by UV light (365 nm UV lamp: VL-4L, Fisher Scientific SAS) and visible light (453 nm LED Spot Luxeon Royal Blue, P453E-PR09, Conrad). All samples were irradiated at a distance of 10 cm from the light source. UV-visible spectra were measured by a Cary 5000 UV-Vis-NIR spectrophotometer (Varian, Inc.). Dynamic light scattering (size) and electrophoretic light scattering (zeta-potential) measurements of the microgel particles was performed with a Zetasizer Nano ZS (Malvern Instruments Ltd.) at angle of 173°. If not explicitly specified in the text the experiments were carried out at 20 °C.

Acknowledgements

The German Research Council is gratefully acknowledged for financial support via SPP 1259 "Intelligent hydrogels", CoE "UniCat", and IGRTG 1524 "Self-Assembled Soft Matter Nano-Structures at Interfaces".

Received: March 3, 2012
Published online: July 9, 2012

[1] a) A. Richter, G. Paschew, S. Klatt, J. Lienig, K. F. Arndt, H. J. P. Adler, *Sensors* **2008**, *8*, 561; b) K. Kabiri, H. Omidian, M. Zohuriaan-Mehr, S. Doroudiani, *Polym. Compos.* **2011**, *32*, 277; c) N. S. Satarkar, J. Z. Hilt, *Acta Biomater.* **2008**, *4*, 11; d) L. Zha, B. Banik, F. Alexis, *Soft Matter* **2011**, *7*, 5908; e) A. Fernández-Barbero, I. J. Suárez, B. Sierra-Martín, A. Fernández-Nieves, F. Javier de las Nieves, M. Marquez, J. Rubio-Retama, E. López-Cabarcos, *Adv. Colloid Interface Sci.* **2009**, *147–148*, 88.

[2] a) H. Crowther, B. Vincent, *Colloid. Polym. Sci.* **1998**, *276*, 46; b) R. Pelton, *Adv. Colloid Interface Sci.* **2000**, *85*, 1; c) V. Nerapusri, J. L. Keddie, B. Vincent, I. A. Bushnak, *Langmuir* **2006**, *22*, 5036; d) C. Zhao, P. He, C. Xiao, X. Gao, X. Zhuang, X. Chen, *J. Appl. Polym. Sci.* **2012**, *123*, 2923.

[3] a) S. Sershen, G. Mensing, M. Ng, N. Halas, D. Beebe, J. West, *Adv. Mater.* **2005**, *17*, 1366; b) G. Chen, F. Svec, D. R. Knapp, *Lab Chip* **2008**, *8*, 1198; c) S. Ghosh, C. Yang, T. Cai, Z. Hu, A. Neogi, *J. Phys. D* **2009**, *42*, 135501; d) N. S. Satarkar, W. Zhang, R. E. Eitel, J. Z. Hilt, *Lab Chip* **2009**, *9*, 1773.

[4] a) N. Peppas, J. Hilt, A. Khademhosseini, R. Langer, *Adv. Mater.* **2006**, *18*, 1345; b) Y. Guan, Y. Zhang, *Soft Matter* **2011**, *7*, 6375.

[5] a) S. Nayak, H. Lee, J. Chmielewski, L. A. Lyon, *J. Am. Chem. Soc.* **2004**, *126*, 10258; b) A. G. Skirtach, C. Dejugnat, D. Braun, A. S. Susha, A. L. Rogach, W. J. Parak, H. Mohwald, G. B. Sukhorukov, *Nano Lett.* **2005**, *5*, 1371; c) K.-H. Liu, T.-Y. Liu, S.-Y. Chen, D.-M. Liu, *Acta Biomater.* **2008**, *4*, 1038; d) C. Brazel, *Pharm. Res.* **2009**, *26*, 644.

[6] J. Retama, B. Lopez-Ruiz, E. Lopez-Cabarcos, *Biomaterials* **2003**, *24*, 2965.

[7] Y. Liu, M. Zhu, X. Liu, W. Zhang, B. Sun, Y. Chen, H. Adler, *Polymer* **2006**, *47*, 1.

[8] M. Kokabi, M. Sirousazar, Z. M. Hassan, *Eur. Polym. J.* **2007**, *43*, 773.

[9] A. M. Gobin, D. P. O'Neal, D. M. Watkins, N. J. Halas, R. A. Drezek, J. L. West, *Lasers Surg. Med.* **2005**, *37*, 123.

[10] N. Ravi, H. A. Aliyar, P. D. Hamilton, *Macromol. Symp.* **2005**, *227*, 191.
[11] a) A. Z. Pich, H. J. P. Adler, *Polym. Int.* **2007**, *56*, 291; b) A. O. Govorov, H. H. Richardson, *Nano Today* **2007**, *2*, 30; c) P. Schexnailder, G. Schmidt, *Colloid. Polym. Sci.* **2009**, *287*, 1; d) N. S. Satarkar, D. Biswal, J. Z. Hilt, *Soft Matter* **2010**, *6*, 2364.
[12] G. Chen, F. Svec, D. R. Knapp, *Lab Chip* **2008**, *8*, 1198.
[13] T. Satoh, K. Sumaru, T. Takagi, T. Kanamori, *Soft Matter* **2011**, *7*, 8030.
[14] M. Bradley, B. Vincent, N. Warren, J. Eastoe, A. Vesperinas, *Langmuir* **2006**, *22*, 101.
[15] K. Kratz, T. Hellweg, W. Eimer, *Colloids Surf. A* **2000**, *170*, 137.
[16] a) A. Burmistrova, R. von Klitzing, *J. Mater. Chem.* **2010**, *20*, 3502; b) M. Karg, I. Pastoriza-Santos, B. Rodrigues-Gonzalez, R. von Klitzing, S. Wellert, T. Hellweg, *Langmuir* **2008**, *24*, 6300.
[17] a) A. Burmistrova, M. Richter, C. Uzum, R. von Klitzing, *Colloid. Polym. Sci.* **2011**, *289*, 613; b) A. Burmistrova, M. Richter, M. Eisele, C. Uzum, R. von Klitzing, *Polymers* **2011**, *3*, 1575.
[18] K. Fan, M. Bradley, B. Vincent, *J. Colloid Interface Sci.* **2012**, *368*, 287.
[19] *Smart light-responsive materials: azobenzene-containing polymers and liquid crystals*, (Eds: Y. Zhao, T. Ikeda) Wiley, Hoboken, NJ **2009**.
[20] Y. Zakrevskyy, A. Kopyshev, N. Lomadze, E. Morozova, L. Lysyakova, N. Kasyanenko, S. Santer, *Phys. Rev. E* **2011**, *84*, 021909.
[21] Y. Zakrevskyy, J. Roxlau, N. Lomadze, G. Brezesinski, S. Santer, unpublished.